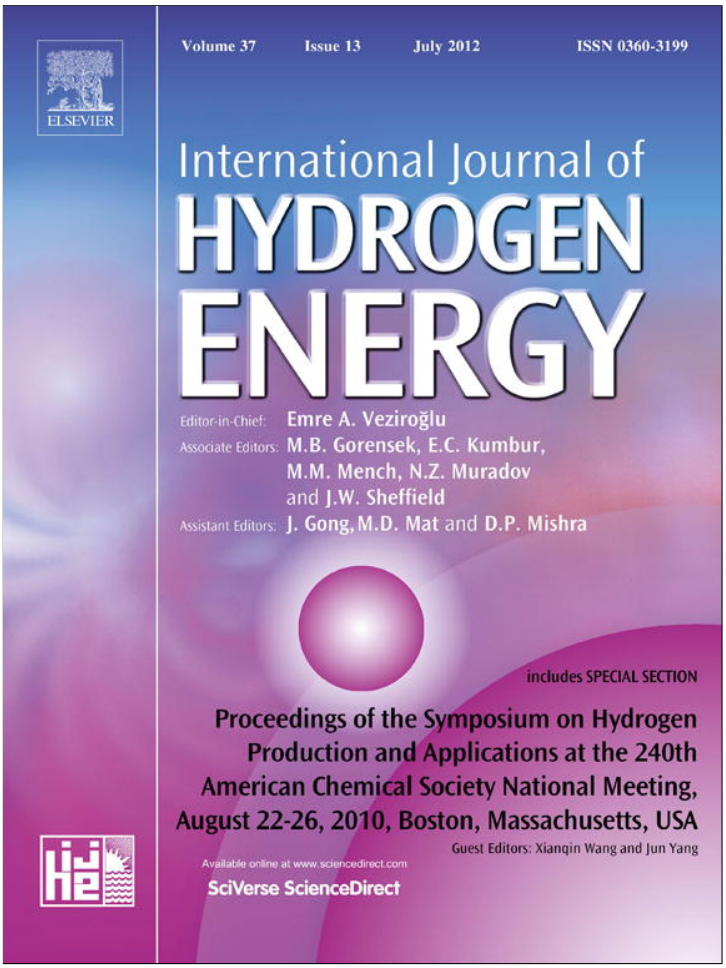

INTERNATIONAL JOURNAL OF HYDROGEN ENERGY 37 (2012) 10346–10353

Available online at www.sciencedirect.com

SciVerse ScienceDirect

journal homepage: www.elsevier.com/locate/he

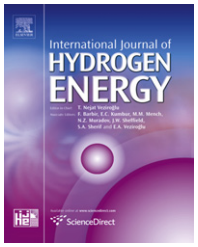

Experimental platform for development and Evaluation of hybrid generation systems based on fuel cells

J.I. Talpone [a,*], P.F. Puleston [a], J.J. More [a], R. Griñó [b], M.G. Cendoya [a]

[a] Consejo Nacional de Investigaciones Científicas y Tecnológicas (CONICET), U.N.L.P, Facultad de Ingeniería, LEICI, Calle 1 y 47, 1900 La Plata, Buenos Aires, Argentina

[b] U.P.C, Escola Tècnica Superior d'Enginyeria Industrial de Barcelona, IOC, Av. Diagonal 647, 08028 Barcelona, Spain

ARTICLE INFO

Article history:
Received 11 September 2011
Received in revised form
4 January 2012
Accepted 31 January 2012
Available online 16 March 2012

Keywords:
Hybrid system
Alternative energy
Fuel cell
Supercapacitor

ABSTRACT

An experimental hybrid power generation platform for the design and assessment of advanced control systems has been developed. It is specifically intended as a flexible development tool for the implementation and refinement of real-time novel control algorithms, aimed to maximize energy efficiency and optimize the electrical power management of hybrid generation systems based on fuel cells. The platform consists of two generation modules and storage module. The main one is based on a PEM fuel cell stack. The second one, implemented with a programmable electronic source, allows to emulate an alternative energy module, particularly a wind energy generation system. The storage module is built with Supercapacitors. Finally, a variable electronic load represents the lumped energy demand, with profiles that can be programmed in accordance with the user requirements. All modules of the system are connected to a common DC bus through intermediary electronic converters, which are controlled by a dedicated digital signal processor. The complete system is supervised through a Personal Computer, resulting into a highly versatile platform. Experimental results are presented to validate the whole system performance.

1. Introduction

The creation of efficient power generation systems based on alternative energy sources has become today an area of important research and development. The growing energy demand, the depletion of fossil fuel resources and the concern about environmental damage have turned attention to technologies based on alternative clean energy sources, particularly those whose availability is continuous and its environmental impact is minimal.

In this way, research in the field of new technologies for hybrid systems has become a high priority issue. In particular, hybrid Decentralised Electrical Generation Systems that incorporate renewable energy sources with a hydrogen/fuel cells generation modules, are of particular interest. Hydrogen can be produced from renewable energies and, when required, converted into electric power by means of fuel cells (FC) [1,2] The capability to store considerable amounts of energy through hydrogen gives more significance to such hybrid generation system topologies. Therefore, hydrogen fed fuel

* *Corresponding author*. Tel.: +54 (0) 221 155643971.
E-mail addresses: juan.talpone@ing.unlp.edu.ar (J.I. Talpone), puleston@ing.unlp.edu.ar (P.F. Puleston), jmore@ing.unlp.edu.ar (J.J. More), roberto.grino@upc.edu (R. Griñó), cendoya@ing.unlp.edu.ar (M.G. Cendoya).
0360-3199/$ – see front matter
doi:10.1016/j.ijhydene.2012.01.161

cells contribute a great deal of flexibility to hybrid decentralised systems and, properly controlled, they can attain high conversion efficiency, remarkable dynamic behaviour and non-polluting emissions. In this context, Proton Exchange Membrane (PEM) Fuel Cells is a promising technology. Their high power density, low operating temperature, solid electrolyte, fast start-up and low sensitivity to orientation make them appropriate for a wide range of applications (from transport to stationary generation) [3,4]. However, PEM fuel cells have serious operation problems and to take up the challenge it is indispensable a great deal of multidisciplinary efforts, coming from electrochemistry, materials technology, fluid-dynamics, thermodynamics, automatic control and electronics. The expected contribution from the control field is twofold. On the one hand, to develop advanced and specialised control systems to have more efficient, safer and long lasting stacks. On the other, in many applications, energy storage devices (Batteries or Supercapacitors) are integrated to the stack, mitigating its exposure to fast loads and endowing more versatility to the system [5]. In these cases, a comprehensive proficient supervisor control is necessary to coordinate the subsystems of the hybrid generation system [6].

In this context, the present work was carried out within the framework of an international collaborative project with the ACES Group of institutes IRII (CSIC-Polytechnic University of Cataluña) and IOC (Polytechnic University of Cataluña), Spain. The key aim of the project is the development of new control strategies and set-ups to maximise energy conversion efficiency and optimize the electrical power management. Specifically, the results of this project phase presented in the paper focuses on the design and implementation of a highly versatile laboratory's generation hybrid test-bench, for real-time analysis, development and experimental assessment of new advanced controllers for such renewable energy based hybrid systems.

2. Laboratory fuel cell based hybrid generation system

2.1. System description

The implemented fuel cell based hybrid system consists of two generation and one storage modules (see schematic in Fig. 1). The main generation source is a fuel cell stack. The second one, implemented with a programmable electronic source (PES), allows to emulate an alternative power generation module, particularly a wind energy generation system. The storage module is built with Supercapacitors (SC). Finally, a variable electronic load (PEL) represents the lumped energy demand, with profiles that can be programmed in accordance with the user requirements.

All modules of the system are connected to a common DC bus through intermediary electronic converters, which are controlled by a dedicated digital signal processor. The DC bus based topology does not require any synchronism or reactive power control as in the case of systems linked by an AC bus. The voltage selected for the bus is 75 V due to equipment compatibility and safety considerations.

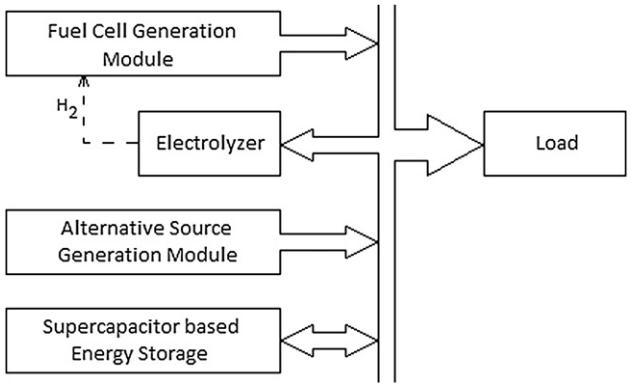

Fig. 1 – System Topology.

2.2. Fuel cell generation module

The Fuel Cell module or main generation module of the developed hybrid platform primarily consists of a FC stack and an electronically controlled power converter (see a block diagram in Fig. 2).

2.2.1. Fuel cell stack

The FC stack generation system is based on PEM fuel cell technology. This technology has been chosen for being the best type of FC candidate for manifold residential and commercial applications, due to their particular features (e.g., low operating temperature, quick start up and high power density). The open circuit voltage of a single PEM cell is in the range of 0.8–1.2 V. To get higher operating voltage and power, many such cells are connected in the form of cascaded series and parallel connection [7,8]. Normally the commercial fuel cell stack gives operating voltage in the range of 12 V–50 V. These class of stacks are adequate to supply smooth power demands, but unsuitable for abrupt load changes due, to slow response of underlying electrochemical and thermodynamic processes [9].

In particular, the proposed FC module has been built around one of this commercial FC stacks, namely a 1.2 kW NEXA®, model MAN5100078, manufactured by Ballard®. The fuel cell stack output voltage can be operated safely in the linear range of voltages from 26 V to 36 V and currents from 10 A to 45 A, for constant hydrogen input fuel supply. Fig. 3 shows the measured output characteristics of the NEXA® 1.2 kW PEM fuel cell model [10].

It can be observed that between the active region and concentrations region there is an approximate linear slope, this is mainly due to the internal resistance offered by various components of the fuel cell. This region is generally referred as Ohmic region [11,12]. The linearized output voltage due to its ohmic nature is given by Eq. (1).

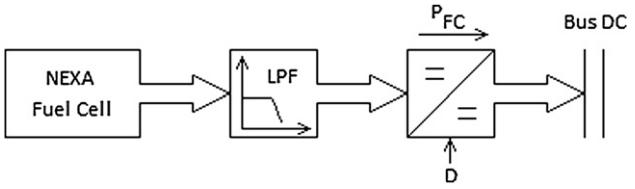

Fig. 2 – Fuel Cell Module.

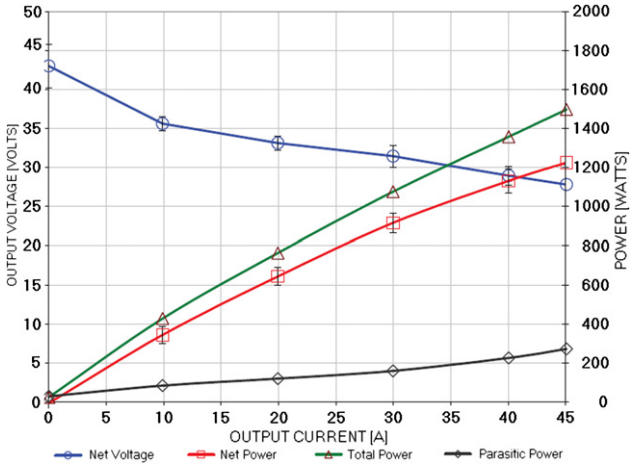

Fig. 3 – NEXA Output Characteristics.

$$V_{FC(lineal)} = V_{0(lineal)} - I_{FC} \cdot R_{internal(lineal)} \quad (1)$$

Note that beyond the linear region, the fuel cells cannot be operated, as electrolyte membrane of the cell may get damaged.

2.2.2. *FC power converter*

The DC-DC converter is an integral part of fuel cell power conditioning unit. The design of DC-DC converters plays an important role to control power regulation particularly sharing a common DC bus [13]. The connection of the stack to the DC bus is done through a step-up (non-isolated) DC-DC unidirectional current converter, so power can only flow from the FC. The selection of such boost converter obeys to its higher efficiency and less component count compared to other DC-DC converter topologies like push pull, half bride and full bridge etc. which could possibly be used to interface fuel cell system to the load.

The boost converter turns the unregulated voltage into desired regulated voltage by varying the duty cycle at high switching frequency lowering the size and cost of energy storage components (a schematic diagram is shown in Fig. 4).

A key topic of its design is the appropriate selection of the inductor and capacitor values, to reduce the ripple generation for a given switching frequency. At this point, note that an issue of careful attention for the designer is the inductor sizing, since being place in the low voltage side, it could result voluminous due to the high currents involved [14].

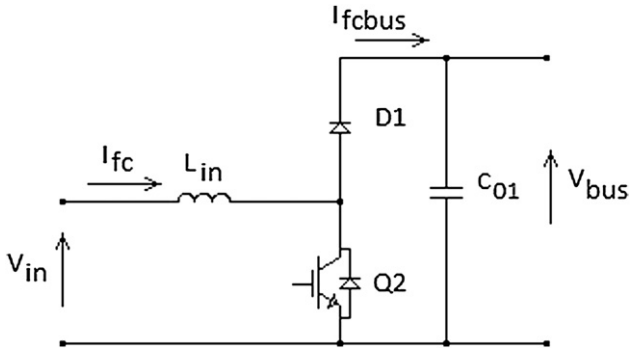

Fig. 4 – Fuel Cell Converter.

For the converter design, the linear region operation of the fuel cell stack is only taken into account. From the characteristic of the FC shown in Fig. 3, the requirements of the converter are specified:

- Input voltage: 26 V–36 V.
- Input current: 10 A–45 A.
- Output voltage: 75 V.
- Maximum power: 1.2 kW.

The first step in the converter design is the determination of the most adequate switches for implementation. After a thorough analysis of possible devices, a Semikron® IGBT commercial module of three columns, usually used to implement power inverters [15], has been selected. The main reason for this choice is that it simplifies the design because it includes many of the elements necessary to build the converter. It incorporates switches and associate drivers, a Hall Effect sensor on each column to measure the FC current (I_{FC}) and the protection logic necessary to prevent simultaneous activation of both switches in a column. The switches control is done through two independent logic signals, allowing the user to choose the appropriate modulation scheme. In addition, each column has two switches of 1200 V to 75 A capability, so one column is enough to implement this converter, leaving the rest available to be used for other modules of the hybrid platform.

The ideal conversion ratio for this converter for continuous conduction mode is:

$$V_{bus} = \frac{V_{in}}{(1-D)} \quad (2)$$

where:

D: duty cycle.
V_{in}: input voltage.
V_{bus}: output voltage.

Knowing the operating region (i.e., the lineal zone) of the FC and taking into account Eq. (2), the range of variation of the duty cycle is established: $0.52 < D < 0.64$. The critical inductance $L_{in(crit)}$, necessary to ensure continuous conduction mode, can be determined from the following expression:

$$L_{in(crit)} = \frac{D \cdot (1-D)^2 V_{bus}}{2 \cdot f_s \cdot I_{fcbus}} \quad (3)$$

where:

f_s: switching frecuency.
I_{fcbus}: output current.

Considering the switching frequency chosen and the above data, the critical inductance value is 22 μHy. Then, L_{in} must be design greater than $L_{in(crit)}$ to guarantee continuous conduction throughout the whole operation range. So, it was decided to use an inductance of 35 μHy, built from the largest acceptable core, given the available materials, size and cost [14].

For this inductance, the maximum ripple obtained is $\Delta I_{FC} = 22$ A given by Eq. (4).

$$\frac{\Delta I_{FC}}{I_{FC}} = \frac{D\cdot(1-D)^2\cdot R}{L\cdot f_S} \tag{4}$$

Considering a maximum accepted V_{bus} voltage ripple of 1%, the lowest value necessary to C_{01}, calculated from Eq. (5) results in 2000 μF [16].

$$\frac{\Delta V_{FC}}{V_{FC}} = \frac{D}{R\cdot C\cdot f_S} \tag{5}$$

Note that, even though the converter will operate in continuous conduction mode over the whole operation range, the input current ripple is significant because the inductance value is close to the critical one. In this sense, recent research studies show that the current ripple affects the normal operation of PEM fuel cells [17]. They conclude that the effect depends on the ripple's frequency and amplitude. Therefore, regarding the ripple's amplitude, in this case, it was necessary to add a low-pass filter between the FC and the power converter. In Fig. 5 is shown the filter's schematic and its connection to the FC and the step-up. It is a second order LC filter whose components were sized based on Eq. (6) & Eq. (7).

$$f_c = \frac{1}{2\cdot\pi\sqrt{L_f\cdot C_f}} \tag{6}$$

$$\zeta = \frac{1}{2\cdot R}\sqrt{\frac{L_f}{C_f}} \tag{7}$$

where:

f_c: cut-off frecuency.
R: filter's equivalent load resistance.
L_f: filter inductance.
C_f: filter capacitance.
ζ: damping factor.

Specifying an attenuation of 60 dB at f_s, then f_c is approximately 500 Hz. From Eq. (6) and Eq. (7) and with $R = 36$ V/10 A = 3.6 Ω, then $L_f = 40$ μHy–60 A and $C_f = 2200$ μF–100 V were obtained. Considering C_f an electrolytic type capacitor, a metalized polyester capacitor $C_p = 1$ μF was added in parallel connection to improve the filter performance at high frequencies.

A final comment regarding the converter implementation. If a particular application requires lower conduction losses, note that for the operating voltage and current ranges power MOSFET switches are suitable instead of IGBTs [19]. However, it should be considered that it is difficult to find in the market similar three columns power modules based on MOSFETs; so the designer should develop and build all the associate hardware necessary to excite the switches and their protections.

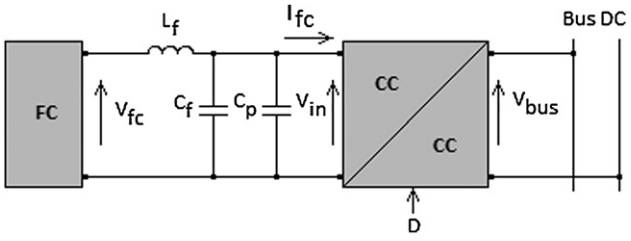

Fig. 5 – Fuel Cell Filter Connection.

2.3. *Supercapacitor storage module*

To complement the Fuel Cell Generation Module, a module comprising energy storage devices such as batteries, capacitors and Supercapacitors is required, particularly to meet the peak power demands and to store possible energy surplus in the hybrid system. Among these energy storage devices, considering the slow response of the FC to changes in power demand, the Supercapacitors are the most suitable due to their fast response to this condition. In this implemented system the Supercapacitor has been linked to the bus through an intermediary DC-DC bidirectional electronic converter. In this way power flow management can be made during charging and discharging conditions (Fig. 6 shows a block diagram of the storage module).

2.3.1. *Supercapacitor sizing*

Considering the requirements mentioned above, the most demanding operating condition corresponds to the case in which the Supercapacitor must provide constant power over a finite time interval. Particularly, the NEXA® stack start-up, corresponding to 2 min [10] and assuming that at this time load should never exceed 500 W (or, equivalently, 1 kW over 1 min). With the specification mentioned, it is possible to provide this power if the SC has been previously fully charged.

A Supercapacitor's voltage profile (voltage vs. time) has two components: a capacitive component, and a resistive component. The capacitive component represents the voltage variation due to the energy change within the Supercapacitor. The resistive component represents the voltage drop due to the equivalent series resistance (ESR) of the Supercapacitor.

The total voltage change when charging or discharging a Supercapacitor includes both of these components. Combining the capacitive and resistive components we obtain Eq. (8).

$$\Delta V = i\cdot\frac{\Delta t}{C_{SC}} + i\cdot R \tag{8}$$

where:

ΔV: the change in voltage during the discharge of the capacitor.
i: the current during the discharge of the capacitor.
Δt: the duration (in seconds) of the discharge pulse.
C_{SC}: the capacitance of the Supercapacitor system at its operating point.

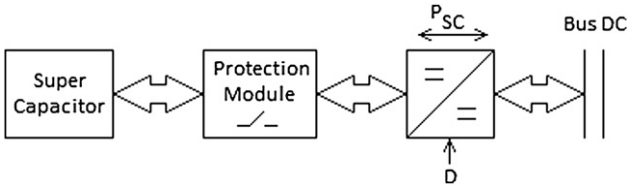

Fig. 6 – Supercapacitor Storage Module.

In analysing any application, is first need to determine the system variables. From these, we determine the value of the variables required to solve Eq. (8). We therefore need to gather the following information about the application.

V_{max}: maximum SC voltage.
V_w: working operating voltage.
V_{min}: minimum allowable voltage.
i: current requirement.
P: power requirement.
t: time of discharge (or charge).

The energy that can be extracted from a Supercapacitor is given by Eq. (9).

$$\Delta E_{SC} = \frac{1}{2}\cdot C_{SC}\cdot\left(V_w^2 - V_{min}^2\right) \quad (9)$$

where:

ΔE_{SC}: energy stored variation.

One commonly used method to size a solution is to determine the optimum size which meets the needed requirements, and then chose based on actual product offerings. The DC bus system's voltage is 75 V. Considering a maximum voltage for the SC of about 2/3 of the bus voltage [19], then $V_{max} = 50$ V. Allowing ΔE_{SC} of 75% of nominal value, then from Eq. (9) $V_{min} = V_w/2$. For safety reasons was chose to work with $V_w = 45$ V. This makes $V_{min} = 22.5$ V [19]. This way these were the requirements needed for the FC sizing:

$V_w = 45$ V.
$V_{min} = V_w/2 = 22.5$ V.
Power = 1 kW.
Time = 60 s.

From the parameters above, the values for the variables in Eq. (8) were determined:

$\Delta V = V_w - V_{min} = 45V - 22.5\ V = 22.5\ V$
$i_{max} = Power/V_{min} = 1000\ W/22.5\ V = 45\ A$
$i_{min} = Power/V_{max} = 1000\ W/50\ V = 20\ A$
$i_{avg} = (45\ A + 50\ A)/2 = 47.5\ A$
$i = 47.5$ A
$\Delta t = 60$ s.

From Eq. (8) and considering an RC Supercapacitor time constant of 1 s [18], since $R^*C = 1$, then $R = 1/C$. Having all the variables defined, rearranging Eq. (8) and solve for C_{SC}:

$$C_{SC} = \frac{i}{\Delta V}\cdot(\Delta t + 1) \quad (10)$$

Substituting in Eq. (10) the values for ΔV, i, and Δt: $C_{SC} = 128$ F.

Considering the specifications mentioned above, it was decided to use a Maxwell® Supercapacitor [15] whose basic characteristics are:

- Capacitance: 165 F.
- Nominal Voltage: 48.6 V.
- Maximum Voltage: 50.4 V.
- ESR: 6.3 mΩ (RC ≈ 1 s).
- Maximum DC current: 98 A.

This model was chosen due to its technical characteristics, cost and market availability.

2.3.2. *Supercapacitor power converter*

This converter was implemented with other Semikron® module column mentioned above and it's structure is shown in Fig. 7. Considering its limitations [15] and the characteristics of the SC, the requirements for the power converter are determined:

- Input Voltage: 22.5 V–45 V.
- Input Current: 0 A–60 A.
- Output Voltage: 75 V.

The switches Q1 and Q2 are complementary. Because, in this case, the current flows both ways, the converter always operates in continuous conduction mode. For availability reasons, for this converter we used the same value of inductance L_{in} as in the unidirectional one for the FC. The duty cycle Eq. (2) is between $0.4 < D < 0.7$. This way, the current ripple results $\Delta I_{sc} = 22.5$ A [16]. In addition, considering Eq. (5) the minimum capacity required to obtain a voltage ripple V_{bus} of about 1% results in 2800 μF [12]. Thus, since both drives share the same DC bus, was decided to integrate C_{01} and C_{02} in a single capacitor bank formed by EPCOS B43303A0687, with an equivalent capacity $C_{bus} = 3720$ μF. This value, if it is necessary, can be easily increased due to the system structure design.

2.3.3. *Supercapacitor protection module*

Given the limitations of the SC and the associated converter, it is necessary to have a protection module to disconnect the SC in case its output voltage reaches the maximum value or the current through the converter's switches is excessive. As shown in Fig. 8, it consists of control logic responsible for measuring the SC's voltage and current at the converter input.

When the system operates normally, the switch S_p remains open and S_s closed. In case the SC's voltage exceeds 48 V or the current reaches ±60 A, the logic closes S_p and opens S_s, connecting a discharge resistor R_d in parallel to the SC and disconnecting it from the converter. Thus, the SC begins to

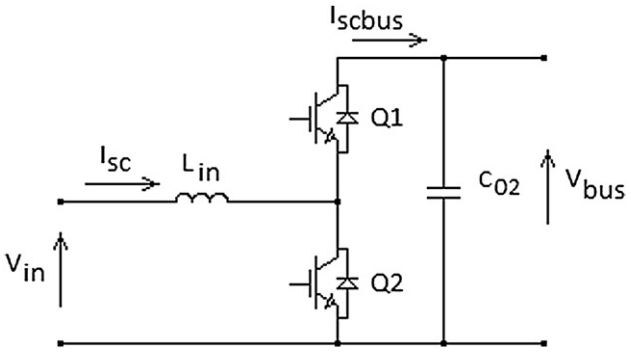

Fig. 7 – Supercapacitor Converter.

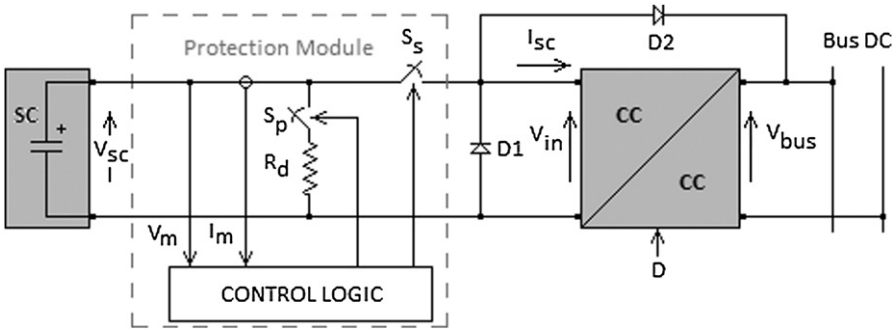

Fig. 8 – SC Protection Module.

discharge. To avoid over voltages caused at the opening of S_s by the converter input inductor, a latch formed by D1 and D2 was placed.

The control logic was implemented using discrete logic instead of a microprocessor because this kind of devices does not ensure that the program, running inside, that monitors all variables of interest is working properly and the operator does not know it. When the protection has been triggered, it must be reset manually by the operator, increasing, this way, the system's security.

2.4. *Alternative generation module*

This module must be able to emulate alternative energy systems (wind, solar, etc.) connected to the DC bus of the hybrid platform. The module must be highly flexible and programmable from a PC. For instance, in the case of wind energy conversion emulation, it must be possible to program different turbine power coefficient characteristics together with wind speed profiles, selected by the user.

For its implementation a 3 kW Electronic Power Source (EPS) made by H&H® was selected, considering the above requirements. The output voltage can reach a maximum of 80 V DC, so it is connected directly to the DC bus. This versatile device allows to control the power injection profile from the PC, processing data either from keyboard or from a stored input file. In addition, voltage or current output modes can be chosen.

2.5. *System load*

A 4.2 kW Programmable Electronic Load (PEL) of the German company H&H® represents the lumped energy demand, with profiles that can be programmed in accordance with the user requirements. In this module the effect of an electrolyzer is also considered. However, the system supports, with minor modifications, the incorporation of a real electrolyzer, when experiments require. The PEL can easily be programmed and monitored by a PC providing great flexibility to change the system load conditions. As the EPS, the PEL is connected directly to the common DC bus.

2.6. *Processing and control module*

The whole system is controlled and monitored by a real time processing unit. Moreover the electronic converters for de FC and SC must be controlled by a real time processing system in order to control their switches precisely. For this application was decided to use a dedicated digital signal processor (DSP) to manage both converters instead of other possible systems such as Microcontrollers, FPGAs or a PC running a real time operating system (RTOS). Microcontrollers should be adequate but it is difficult to execute complex algorithms with them, FPGAs are usually used when high speed acquisition is necessary and a PC running a RTOS is not a "robust" option to control electronic converters when high powers are involved.

The DSP is based on a ® Spectrum Digital DSP development kit that works with a Texas Instruments ® FZ28335 (150 MHz) core. In order to measure and acquire the signals of interest, it was developed a board for signal conditioning and filtering. The variables of interest are:

V_{fc}–I_{fc}: FC voltage and current.
V_{sc}–I_{sc}: SC voltage and current.
V_{bus}–I_{bus}: Bus voltage and current.

These signals are filtered and conditioned for the DSP analog to digital conversion module. This way, the DSP acquires the above signals and executes in real time the user control algorithms, determining the status for each converter switches instantaneously. The advantage of the development board used is that it can be programmed using MATLAB® Simulink®. This characteristic provides the system high versatility and allows the user easy programming.

The system's supervisor control is performed by a PC. It is connected to the DSP via a USB interface. This way they can exchange control and measurement parameters of the system. It is also responsible for generating the power profile for the additional generation channel (injection) and the set the Load condition. The PC displays and stores the voltages and currents measurements of the system. The user can run/stop the DSP, change parameters and configure the PEL and PES, and know the operating conditions of the platform at any time using the PC.

3. Experimental results

Experimental results of an example application for the platform developed in this work are presented in this section. The control objective is to maintain the DC common bus voltage at

60 V. The Fuel Cell is responsible for providing the low-frequency component of the power demanded by the load. The SC is responsible for supplying the power transients, to a change in the power demand during the time interval while the FC reaches the new value requested by the load. For this purpose the SC converter is controlled by two loops: an inner current loop, and an exterior voltage one to regulate the 60 V DC voltage on the bus.

The FC converter is controlled by a current loop whose reference is calculated from the power demanded by the load. In the calculation of this reference is also considered the voltage error of the SC so that it recharges slowly to a safety operation value of 42 V. Fig. 9 shows the curves obtained from the test performed. I_{bus} and V_{bus} are shown in blue, I_{SC} and V_{SC} in red, and I_{FC} and V_{FC} in green respectively. I_{bus} corresponds to the resultant load current: $I_{bus} = I_{load} + I_{electrolyzer} - I_{alternative\_source}$.

Initially, the FC and SC current loops are closed and a 4 A reference is set in the SC to charge it until its voltage is about 15 V at t_1. At this time the DC bus voltage loop is closed with a 60 V reference. The current reference value of the FC is also increased and SC is still left charging.

The power demand is increased at t_2 being initially provided by the SC. At t_3 the reference value for the FC's current loop starts to being calculated from the load power demanded and that required by the SC to maintain its voltage at 42 V. Finally, at t_4, when the load power demand increases again, it can be seen how initially it's provided by the SC until the FC reaches the new stationary value and can supply it.

Currents I_{FC} (blue in the web version) and I_{SC} (green in the web version) are shown in Fig. 10. It can be seen that the currents ripple in both cases meet the design specifications. In addition, the current corresponding to FC converter indicates that it is operating in discontinuous conduction mode while that for the SC operates in continuous conduction with average current close to zero.

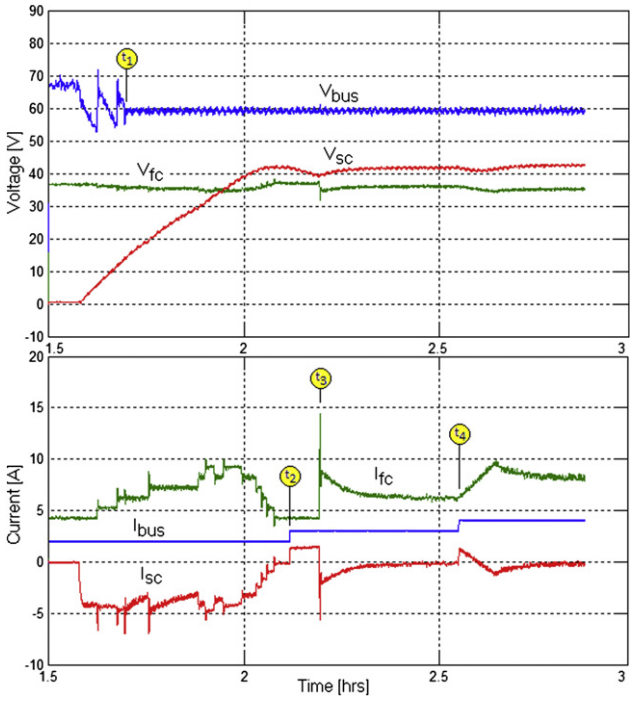

Fig. 9 – Experimental Results.

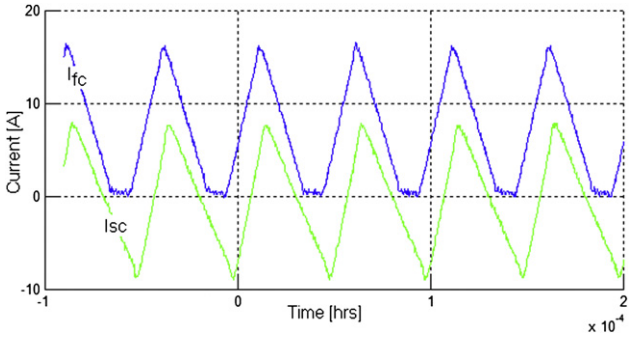

Fig. 10 – Converters Currents.

4. Conclusions

This work detailed the main guidelines for the development of an experimental versatile hybrid generation platform based on a commercial Fuel Cell stack and a Supercapacitors bank. The main design guidelines for construction and operation of the whole system were described. Special attention was given to the design and implementation of the electronic converters, instrumentation, control & supervision, and protection systems. The platform was tested demonstrating the correct operation for the test conditions imposed.

REFERENCES

[1] Balat Havva, Kirtay Elif. Hydrogen from biomass – present scenario and future prospects. International Journal of Hydrogen Energy July 2010;35(14):7416–26. doi:10.1016/j.ijhydene.2010.04.137. issn:0360-3199.

[2] Dönitz W. Fuel cells for mobile applications, status, requirements and future application potential. International Journal of Hydrogen Energy July 1998;23(7):611–5. doi:10.1016/S0360-3199(97)00075-X. issn:0360-3199.

[3] Khorrami F, Puranik S, Keyhani A, Krishnamurthy P, and She Y. PEM fuel cell distributed generation system: modeling and robust nonlinear control. In 48th IEEE Conference on Decision and Control conference, Shanghai, Dec. 16–18, 2009.

[4] Lee H-S, Jeong K-S, Oh B-S. An experimental study of controlling strategies and drive forces for hydrogen fuel cell hybrid vehicles. International Journal of Hydrogen Energy 2003;28:215–22.

[5] Kisacikoglu MC, Uzunoglu M, Alam MS. Load sharing using fuzzy logic control in a fuel cell/ultracapacitor hybrid vehicle. International Journal of Hydrogen Energy 2009;34(3):1497–507.

[6] Suh K-W, Stefanopoulou AG. Coordination of converter and fuel cell controllers. International Journal of Energy Research 2005;29(12):1167–89.

[7] Farooque Mohammad, Maru Hans C. Fuel cells-the clean and efficient power generators. Proceedings of the IEEE December 2001;89(2):1819–29.

[8] Ellis Michael W, Von Spakovsky Michael R, Nelson Douglas J. Fuel cell systems: efficient, flexible energy conversion for the 21st Century. Proceedings of the IEEE Dec.2001;89(12):1808–18.

[9] Hashem Nehrir M, Wang Caisheng, Shaw Steven R. Fuel cells: promising devices for distributed generation. IEEE Power & Energy Jan/Feb. 2006;4:47–53.
[10] Nexa™ (310-0027) Power Module User's Manual, Ballard Power Systems Inc.
[11] Arsov Goce L. Improved Parametric Pspice Model of PEM fuel cell, 11th International Conference on optimization of electrical and electronics equipment; May 2008. pp. 203–208.
[12] Cheng KWE, Sutanto D, Ho YL, Law KK. Exploring the power conditioning system for fuel cell, in 32nd IEEE Annual Power Electronics Specialists Conference; 2001. pp. 2197–2202.
[13] Fernandez LM, Garcia P, Garcia CA, Torreglosa JP, Jurado F. Comparison of control schemes for a fuel cell hybrid tramway integrating two dc/dc converters. International Journal of Hydrogen Energy 2010;35(11):5731–44.
[14] McLyman C. Transformer and inductor design handbook. 2nd ed. Dekker; 1988.
[15] Semikron. Semistack SKS 75F B6CI 40 V12 Datasheet; 20/4/2007.
[16] Mohan N, Undeland TM, Robbins WP. Power electronics converters, applications and design. 3rd ed. John Wiley & Sons; 2001.
[17] Kim Jong-Hoon, Jang Min-Ho, Choe Jun-Seok, Kim Do-Young, Tak Yong-Sug, Cho Bo-Hyung. An experimental analysis of the ripple current applied variable frequency characteristic in a polymer electrolyte membrane fuel cell. Journal of Power Electronics January 2011;11(1).
[18] Maxwell Technologies, Inc. BMOD0165 P048 Datasheet, Document number: 1009365.8.
[19] Maxwell Technologies, Inc. Applications Note: "BOOSTCAP® Ultracapacitor Cell Sizing", Document number: 10073627.